University of Thi-Qar Journal of Science (UTJsci)
E-ISSN: 2709-0256, P-ISSN: 1991-8690, Vol. 13, No. 1, Jun. 2026

Linear Gain of Si / SiO_2 Quantum Dot laser

Amira H. Hussein[1a] and Baqer O. Al-Nashy[1b*]
[1]*Department of Physics, College of Science, University of Misan, Omarah, Iraq*
[a]Email: ameera10@uomisan.edu.iq
[b*]Corresponding author: baqernano@uomisan.edu.iq

Received: 23-07-2025, Revised: 23-08-2025, Accepted: 06-09-2025, Published: 01-06-2026

***Abstract*—Linear Gain spectra of $Si/SiOx$ undoped and doped Quantum Dot laser are studied under the inhomogeneous broadening assumption for four the height disc quantum dot laser are (h=0.2nm,h=0.5nm,h=1nm,h=1.5nm) the disc height QDL size effect on the gain, .the wavelength and the linear gain increase obtained by increase QDL size height and so four the radius at quantum dot are (ρ=8 nm, ρ=10 nm, ρ=12 nm, ρ=16 nm) . we show that disc radius QDL size effect on gain-wavelength relation where at increase QDL radius (ρ=16 nm) the gain lower and shift wavelength amount (15 nm) to right. We studied at four SiO_x mole concentration ($x = 0.11, 0.15, 0.25, 0.35$) for WL (barrier layer) The different concentrations in the SiOx WL layer (mole fractions in the WL), the gain for four SiOx -mole fractions, The gain peak reduced and shifted to down (absorption) for tow curve with increasing SiOx concentration in the WL. The gain for the doped structures doubles the undoped ones. The gain increases while the wavelength is reduced with increasing Cd content due to the broader band discontinuity between QD states. These visible bands are essential in different applications. The effect of QD size effect is also examined. The wavelength is extended by 20 nm for each 1 nm QD height increment**

***Keywords*—silicon -based, Quantum dot, gain, doping, Si/SiOx.**

I. INTRODUCTION

Optical gain is the increase in the proportion of photon density (light intensity) per unit length of light transmission[1]. The optical gain coefficient g is also expressed in inverse centimeters (1/cm), just as the optical absorption coefficient αo**.** When an electron relocates moving from a band with lower energy to one with more energy due to photon absorption, an electron–hole pair is formed. When an existing electron-hole pair is induced to recombine, gain is produced [2]. Producing an additional photon. The amplitude of the monochromatic wave is doubled by the second photon, which has the same wavelength and phase as the first. When this process is repeated, considerable amplification of light results. When the conduction band, which is the higher energy level, contains more electrons, than at the lower energy level, stimulated emission predominates. Valence band level. By supplying valence band holes from the p-doped side and conduction band electrons from the n-doped side, np-junctions can accomplish this inversion of the carrier population[3].There are two types of optical amplifiers are semiconductor optical amplifiers (SOA) and optical fiber amplifiers. Conventional system applications like in-line amplification to compensate for optical connection losses are dominated by the former [4].

silicon is one of the most prevalent elements on Earth [5]. Is a semiconductor with an indirect band gap that has a low likelihood of phonon-assisted, radiative electron-hole recombination, which would cause photons to spontaneously emit [6]. and, when its size approaches the bulk Bohr radius (4 nm for silicon), exhibits notable changes in optical and electrical characteristics [7] Since silicon is considered one of the most important semiconductors widely used in electronics and communications, integrating quantum dots with silicon opens new horizons for enhancing optical and electronic properties and expanding practical applications.

Quantum dots (QDs) have attracted considerable attention from physicists, chemists, and materials engineers over the years due to their fascinating carrier confinement effects. These effects arise when the motion of charge carriers within a solid is limited in certain directions to dimensions comparable to their de Broglie wavelength, leading to discrete energy levels along those dimensions. This quantization of energy levels is especially significant when charge carriers are confined in all three dimensions, as is characteristic of quantum dots [8].

Due to quantum confinement phenomena, quantum dots—nanoscale semiconductor particles that are usually between 2─10 nanometers in size—display special optical and electrical characteristics. Because electrons in quantum dots are restricted to such small dimensions, their energy levels become discrete, much like those of atoms. This enables quantum dots to produce light at specific wavelengths depending on their size [9].

This work studies the optical and electronic properties of the $Si/SiOx$ QD structure lattice-matched to the $SiOx$ barrier. Such a barrier is chosen due to its stability over time compared with other structures. It also has enough bandgap energy to cover (in the energy diagram) the QD structure for metals[10-11]. It is possible to grow Si-based QD structures on nitrides [12].The results in [8-9] approve the possibility of preparing the structures studied in this work. Doped structures are also analyzed. Inhomogeneously broadened gain (which has the characteristics of self-assembled QDs) is considered. The band discontinuity of each band is specified for each mole fraction, which is critical in determining the QD energy states in each band. The gain is doubled with doping. QD size is efficient in changing the

https://doi.org/10.32792/utq/utjsci/v13i1.1454

peak wavelength. The structures studied cover the visible band of essential applications.

II. Linear Optical Gain

The modal optical linear gain per QD layer of the self-organized QDs is then determined by multiplying the gain by the optical confinement factor, which denotes the advantageous portion of the gain.is given by[13]:

$$\Gamma g^{(1)}(\hbar\omega) = \Gamma C_0 \sum_i \int_{-\infty}^{\infty} dE' |M_{env}|^2 |\hat{e}.P_{cv}|^2 \times D(E')L(E',\hbar\omega)[f_c(E',F_c) - f_v(E',F_v)] \quad \text{... [1]}$$

where all of the radiative energy transitions are taken into consideration by calculating the summation *i* over the conduction and valence QD energy subbands. Depended the term $|\hat{e}.P_{cv}|^2$ is the QD momentum matrix element on the light polarization considered with $\hat{e}$ is a unit vector in the polarization direction. The envelope function term $|M_{env}|^2$ is taken between the QD electron and hole energy states that have the same quantum numbers [14].

Considering the parabolic form of the band, the momentum matrices of QDs are taken to be the same as those of QW near the zone center ($k_t = 0$) for heavy hole band and, are expressed as:

$$|\hat{e}.P_{cv}|^2 = \frac{3}{2}(M_b^2) \quad \text{…….. [2]}$$

where the bulk momentum matrix element given by:

$$M_b^2 = E_p \frac{m_0}{6} \quad \text{…... [3]}$$

And E_p is the optical matrix energy parameter, it is given by[15]:

$$E_p = \left(\frac{m_0}{m_e} - 1\right)\left(\frac{E_g.(E_g+\Delta_0)}{E_g+\frac{3}{2}\Delta_0}\right) \quad \text{…... [4]}$$

Where Δ_0 is spin-orbit splitting energy, E_g is the energy gap of the QD and m_0 is the free electron mass.

$$C_0 = \frac{\pi e^2}{n_b c \varepsilon_0 m_0 \omega} \quad \text{... [5]}$$

Where n_b is the material background refractive index, c is the light speed in the free space, ε_0 is the free space permittivity, ω is the optical angular frequency and e *is* the electron charge [16].

The self-assembled QDs state density with inhomogeneous broadening is determined by [13].

$$D(E') = \frac{s^i}{V_{dot}^{eff}} \frac{1}{\sqrt{2\pi\sigma^2}} exp\left(\frac{-(E'-E_{max}^{i2}}{2\sigma^2}\right) \quad \text{…….. [6]}$$

s^i represents the degree of degeneracy at each energy state of the QD.

E_{max}^i is the transition energy at the peak of QD distribution of the optical transition energy. σ is the spectral variance of the QD distribution.[13]

Using the quantum disc model to determine the energy states of the QDs after they have taken the shape of a disc. This model is described well in[17]'[18].

In this model, $s^i = 2$ for the QD ground energy state and $s^i = 4$ for the QD excited energy states. Considering that the average height of QDs is h and their areal density is N_D. The effective volume of the QDs represents of V_{dot}^{eff} In the following equation:

$$V_{dot}^{eff} = \frac{h}{N_D} \text{ ... [7]}$$

the optical transition energy brought on by the optical recombination of the heavy hole and electron states QD[15]. The gain spectrum Lorentzian line shape function is provided by;

$$L(E',\hbar w) = \frac{\frac{\hbar\gamma_{cv}}{\pi}}{(E'-\hbar\omega)^2+(\hbar\gamma_{cv})^2}.. \quad \text{…… [8]}$$

$$\hbar\gamma_{cv} = \frac{\hbar}{\tau_{in}} \quad \text{..... [9]}$$

The τ_{in} is the polarization relaxation time considered for the homogeneous broadening of the gain spectrum.

carriers scattering like electron-phonon and electron-electron scatterings. Note that the relaxation time constants are termed by τ_c and τ_v for electrons and holes.

The homogeneous linewidth given by the equation:

$$\hbar\gamma_{cv} = \frac{(\hbar\gamma_{cc}+\hbar\gamma_{vv})}{2} + \hbar\gamma_{ph} \quad \text{…... [10]}$$

The term $\hbar\gamma_{ph}$ takes the pure dephasing case of carrier interactions, where the change is undertaken in the phase (momentum) of the scattered carrier while its energy is conserved. The value of Γ_3 is about 0.7 where the Gaussian distribution was used to approximate the transverse field distribution [19].

A self-organized QD's modal optical nonlinear gain per QD layer is determined by [20]:

In the QD-SOA, the active region represented by width w and thickness d.

III. Results and Discussion

The tables exhibit calculate of energy levels for quantum dot laser and barrier layer, first table we accounted of energy levels at disc radius different, second table show the wavelength and linear gain for each radius in undoped, third table show the wavelength and linear gain for each radius in N-type doped, fourth table show the wavelength and linear gain for each radius in P-type doped.

TABLE 1. Energy Level Change in QD-L size (disc height) Structure Si/SiOx

Energy	$\rho = 8nm$	$\rho = 10$nm	$\rho = 12nm$	$\rho = 16nm$
Energy conduction subbands of (QD)	Ec_1=1.2521eV Ec_2=1.2791 eV Ec_3=1.3280 eV	Ec_1=1.2500 eV Ec_2=1.2677 eV Ec_3=1.2997 eV	Ec_1=1.2488eV Ec_2=1.2613eV Ec_3=1.2839eV	Ec_1=1.2475 eV Ec_2=1.2475 eV Ec_3=1.2547 eV
Energy valance subbands (QD)	Eh_1=0.0067 eV Eh_2=0.0068 eV Eh_3=0.0361 eV Eh_4=0.0887 eV Eh_5=0.1647 eV	Eh_1=0.0043 eV Eh_2=0.0044 eV Eh_3=0.0232 eV Eh_4=0.0571 eV Eh_5=0.1060 eV	Eh_1=0.0030 eV Eh_2=0.0031 eV Eh_3=0.0162 eV Eh_4=0.0398 eV Eh_5=0.0739 eV	Eh_1=0.0017 eV Eh_2=0.0017 eV Eh_3=0.0092 eV Eh_4=0.0225 eV Eh_5=0.0418 eV
Energy conduction subbands of (WL)	2.114 eV	2.1144 eV	2.1144 eV	2.1144 eV
Energy valance subbands of (WL)	6.6170 eV	6.6170 eV	6.6170 eV	6.6170 eV

TABLE 2. The wavelength and gain un-doped for the Structure Si/SiO_x for different dot radius

Radius (ρ)	wavelength(λ)	Gain (1/cm)
ρ =8nm	984.615nm	$5.827 \times 10^3 cm^{-1}$
ρ =10nm	$1 \times 10^3 nm$	$3.045 \times 10^3 cm^{-1}$
ρ =12nm	$1.009 \times 10^3 nm$	$1.743 \times 10^3 cm^{-1}$
ρ =16nm	$1.009 \times 10^3 nm$	$1.133 \times 10^3 cm^{-1}$

TABLE 3. The wavelength and gain N-type doped for the Structure Si/SiO_x for different disc radius

Radius (ρ)	wavelength(λ)	Gain (g)
ρ =8nm	981.818nm	$6.334 \times 10^3 cm^{-1}$
ρ =10nm	$993.939nm$	$3.465 \times 10^3 cm^{-1}$
ρ =12nm	$1.006 \times 10^3 nm$	$1.984 \times 10^3 cm^{-1}$
ρ =16nm	$1.006 \times 10^3 nm$	$1.159 \times 10^3 cm^{-1}$

TABLE 4. Table 4 Radius p-type for the Structure Si / SiO_x

Radius (ρ)	wavelength(λ)	Gain (g)
ρ =8nm	982.857nm	$7.435 \times 10^3 cm^{-1}$
ρ =10nm	$994.286nm$	$4.401 \times 10^3 cm^{-1}$
ρ =12nm	$1.006 \times 10^3 nm$	$2.366 \times 10^3 cm^{-1}$
ρ =16nm	$1.006 \times 10^3 nm$	$1.522 \times 10^3 cm^{-1}$

We have determined the energy levels for the structure Si/SiO_x in the dot layer at the different four heights. This is shown in Table 5, while the tables 6 undoped, 7 N-type doped and 8 P-type doped show the wavelength and gain for each height.

TABLE 5. Energy Level Change in QD-L size (disc height) Structure Si/SiOx

high	$h = 0.2nm$	$h = 0.5nm$	$h = 1nm$	$h = 1.5nm$
Energy valance subbands (QD)	Ec1= 1.9007eV Ec2= 1.9132 eV Ec3= 1.9358 eV	Ec1= 1.5774 eV Ec2= 1.5899 eV Ec3= 1.6125 eV	Ec1= 1.3746 eV Ec2=1.3872 eV Ec3=1.4097 eV	Ec1= 1.2934 eV Ec2= 1.3059 eV Ec3= 1.3285 eV
Energy valance subbands (QD)	Eh1=0.0030 eV Eh2=0.0031 eV Eh3=0.0162 eV Eh4=0.0398 eV Eh5=0.0739 eV	Eh1=0.0030 eV Eh2=0.0031 eV Eh3=0.0162 eV Eh4=0.0398 eV Eh5=0.0739 eV	Eh1=0.0030 eV Eh2=0.0031 eV Eh3=0.0162 eV Eh4=0.0398 eV Eh5=0.0739 eV	Eh1=0.0030 eV Eh2=0.0031 eV Eh3=0.0162 eV Eh4=0.0398 eV Eh5=0.0739 eV
Energy conduction subbands of (WL)	2.1144 eV	2.1144 eV	2.1144 eV	2.1144 eV
Energy valance subbands of (WL)	6.6170 eV	6.6170 eV	6.6170 eV	6.6170 eV

TABLE 6. values the gain and wavelength undoped for the Structure Si/SiO_xat different heights

High(h)	**wavelength(λ)**	**Gain (g)**
h=0.2nm	663.75nm	$1.147 \times 10^3 cm^{-1}$
h=0.5nm	$800.714nm$	$1.53 \times 10^3 cm^{-1}$
h=1nm	$923.75nm$	$1.765 \times 10^3 cm^{-1}$
h=1.5nm	$983.333nm$	$1.868 \times 10^3 cm^{-1}$

TABLE 7. High n-type for the Structure Si / Sio_x

High(h)	**wavelength(λ)**	**Gain (g)**
h=0.2nm	661.429nm	$1.367 \times 10^3 cm^{-1}$
h=0.5nm	$794.805nm$	$1.878 \times 10^3 cm^{-1}$
h=1nm	$914nm$	$2.157 \times 10^3 cm^{-1}$
h=1.5nm	$972.5nm$	$2.287 \times 10^3 cm^{-1}$

TABLE 8. High p-type for the Structure Si / Sio_x

High(h)	**wavelength(λ)**	**Gain (g)**
h=0.2nm	660.976nm	$1.5 \times 10^3 cm^{-1}$
h=0.5nm	$798.182nm$	$1.95 \times 10^3 cm^{-1}$
h=1nm	$916.364nm$	$2.25 \times 10^3 cm^{-1}$
h=1.5nm	$978.049nm$	$2.375 \times 10^3 cm^{-1}$

TABLE 9. Different mole fraction for barrier layer undoped for the structure Si/SiO_x

$Carriar(n_D)$	wavelength(λ)	Gain (g)
$x = 0.35$	$1.004\times 10^3 nm$	$470 cm^{-1}$
$x = 0.25$	$1.004\times 10^3 nm$	$370 cm^{-1}$
$x = 0.25$	$1.004\times 10^3 nm$	$300 cm^{-1}$
$x = 0.11$	$1.004\times 10^3 nm$	$113.333 cm^{-1}$

TABLE 10. Different mole fraction for barrier layer n-type for the Structure Si/SiO_x

$Carriar(n_D)$	wavelength(λ)	Gain (g)
$x = 0.35$	994.444nm	$510 cm^{-1}$
$x = 0.25$	994.444nm	$382.727 cm^{-1}$
$x = 0.25$	994.444nm	$306.364 cm^{-1}$
$x = 0.11$	994.444nm	$115.455 cm^{-1}$

TABLE 11. Different mole fraction for barrier layer p-type for the Structure Si/SiO_x

$x = 0.35$	$1\times 10^3 nm$	$618.75 cm^{-1}$
$x = 0.25$	$1\times 10^3 nm$	$518.75 cm^{-1}$
$x = 0.25$	$1\times 10^3 nm$	$452.632 cm^{-1}$
$x = 0.11$	$1\times 10^3 nm$	$281.818 cm^{-1}$

IV. Quantum Size Effect (QD-L Height)

Figure.3.1 shows the plots of (Gain 1/cm) versus wavelength (height from h=0.2 nm, h=1.5 nm, h=0.5 nm to h=1 nm), the disc height QDL size effect on the gain, .

Fig. 1(A) un-doped Si/SiO_x system, shorter wavelength and the linear gain are obtained by decreasing QDL size height. For every 0.5 nm drop in height, the wavelength is shortened by about 60 nm and the gain is decrease by 75 cm^{-1}. The gain peak increase and shifted to longer wavelength with increasing Si/SiO_xQD-L height size.

Fig. 1(B) explain p-type doped for QDL size (height), each curve or spectrum change absorption state to the gain where is high linear gain when h=1.5 nm and high gain and far shift wavelength while h=0.2 nm decrease linear gain and reduced wavelength , show increase in the gain and shifted to longer wavelength with increasing dot height A comparison done in Table 1 shows that the main change in the spectrum is obtained by changing disc height in the QDL layer.

This is due to reducing barrier potential in the dot layer, i.e. increasing carrier confinement for the overall system. when QD height in the layer increased by (1 nm), the wavelength is green solid line shifted by ~80 nm, we assume that the homogeneous linewidth due to gain recovery is the same as the linewidth due to pure dephasing.

Fig. 1(C) n-type doped at different system the experimental and theoretical observations where it is found that the variation between conduction- valence-band ground state energies is more sensitive to the height fluctuation than the change of base. red dash line gives lower gain and shorter wavelength than other spectra (Red dash line, blue dash line, black dash line) due to QD size effect (where at decrease dot height) while black dash line have bigger gain and longer wavelength. wavelength shift for red dash line (450 to 550) compared blue dash line (500 to 650 nm), we noted when increase dot height increase gain and wavelength. green dash line the peak gain covers the (60**0** − 65**0** ***nm*** wavelength) range, black dash line the peak gain covers the (50**0** − 70**0** ***nm*** wavelength) range.

green dash line the peak gain covers the (300 − 360 ***nm*** wavelength) range and black dash line the peak gain covers the (100 ***nm*** wavelength) range. p-type doped QDs with high barrier potential will have a smaller homogeneous linewidth than n-doped QDs with low barrier potential. shows the gain at different QD heights (h), where the peak wavelength is red-shifted with increasing height. The wavelength shift due to increasing height is more than that due to mole fraction change. The wavelength is extended to 6.58 μm when h = 0.2

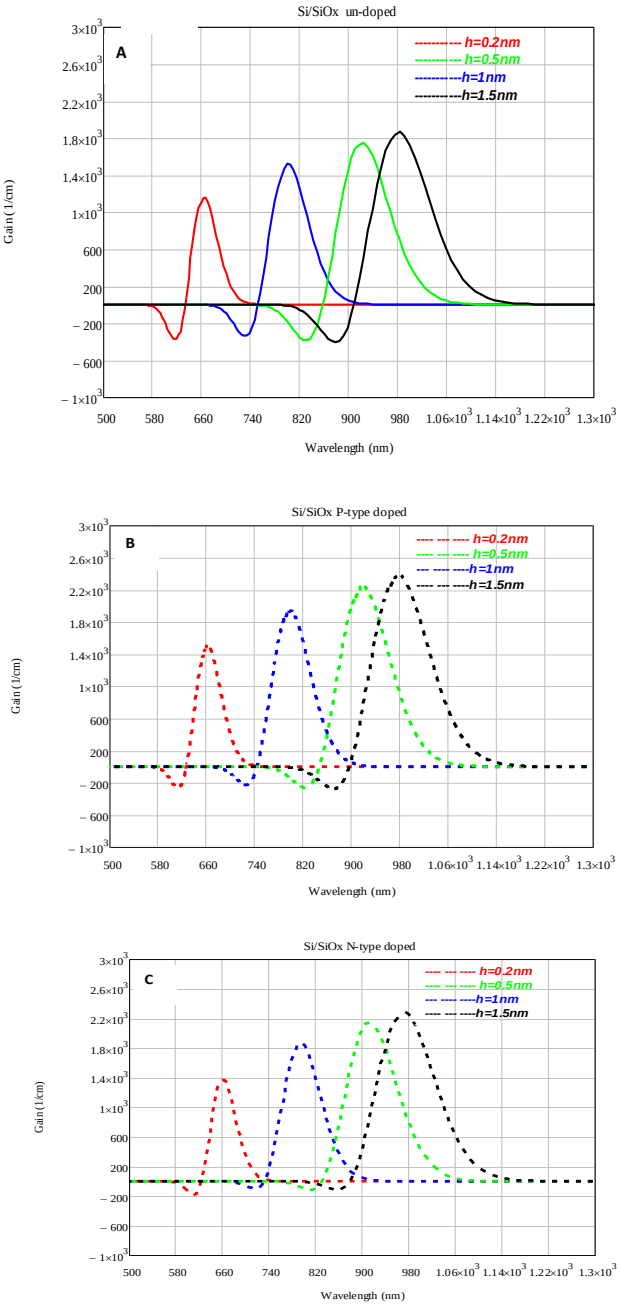

Fig.1: Calculated Gain Spectra at Different Values Of, QD-L Disc Height for Structure Si/Sio$_x$, (A) Spectra of an un-doped Structure is dash line (B) P-type doped Structure is solid line (C) N-type doped structure is solid line

V. Quantum Size Effect (QD-L Radii)

Figure .2 show that disc radius QDL size effect on gain-wavelength relation (ρ=8 nm, ρ=10 nm, ρ=12 nm and ρ=16 nm). where at increase QDL radius (ρ=16 nm) the gain lower and shift wavelength amount (15 nm) to right.

Fig. 2 (A) show that gain value for black line curve is (580cm^{-1}) when radius QD is (ρ=16 nm), while the gain value for red line spectrum is bigger (4 time) form black line curve and lower wavelength. The impact of altering the quantum disc radius where there is a slight change in the wave length is depicted in Figure.1. The gain increases by about 200 cm^{-1} for every 1 nm increase in the disc radius, which is the only variation that can be taken into account.

Fig.2 (A) shows the gain spectra of undoped QD radii of Si/SiO$_x$. This is in line with theoretical and experimental findings that show[21] that the difference between valence- and conduction-band ground state energies

Fig. 2 (B) illustrate p-type doped for QD radii of Si/SiO$_x$, for the doped structure, one peaks have the differ height. The bandwidth of the doped peaks is reduced for higher transition peaks. The gain is so high. The spectrum covers 700-2480 nm wavelength.

Fig .2 (C) show the gain spectra versus wavelength for n-type system When radius concentration is increasing from 8 to 16 nm, the peak gain in both TE and TM reduced by 3 times. A neglected change in the wavelength with this few change in the SiO$_x$ in the WL. The wavelength of this group of structures is 990 nm.

The QD spectra are still at the same peak wavelength despite the change of QD-L size radius, which refers to the main effect of the SiO$_x$ barrier that has a wide bandgap compared to that of QD (Si)

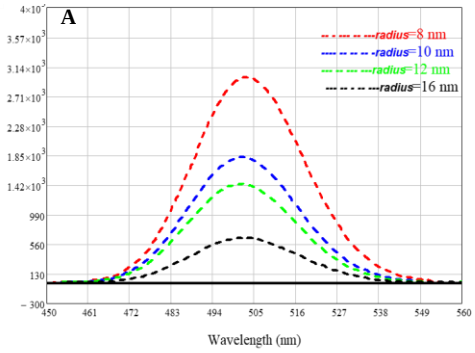

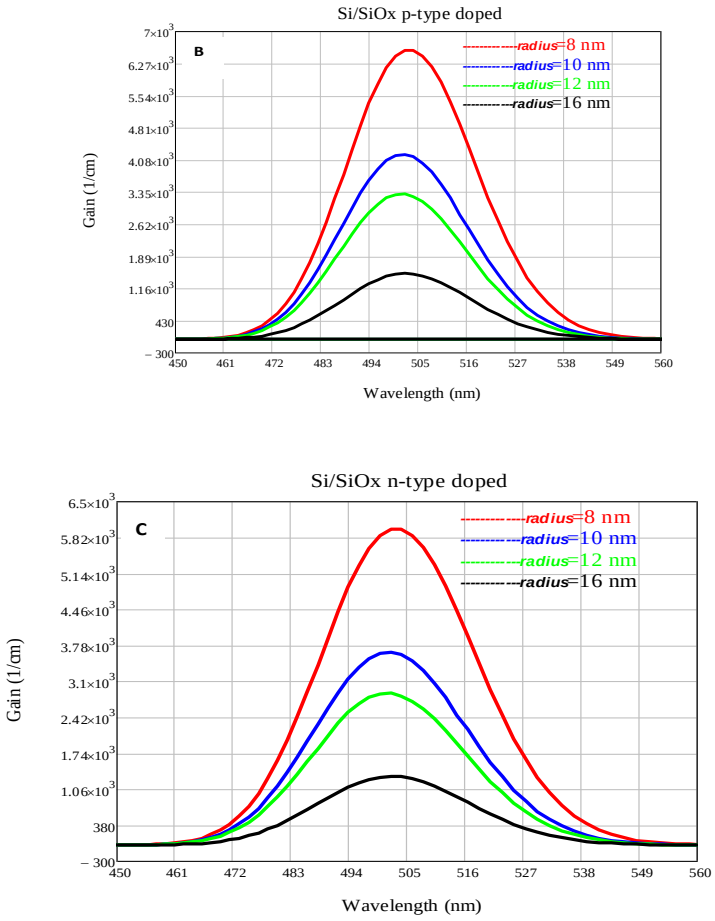

Figure 2: Calculated Gain Spectra at Different Values of, QDL Disc Radii for Structure Si/Sio$_x$, (A) Spectra of An Undoped Structure Is Dash Line And (B) p-type (C) Doped and n-type doped structure is solid line

VI. Concentration Effect WL

Figure .3: shows gain curves vs wavelength for Si/SiO$_x$, system, at different concentrations in the SiO$_x$ WL layer (mole fractions in the WL), the gain for four SiO$_x$ -mole fractions, (0.11, 0.15, 0.25 and 0.35). The gain peak reduced and shifted to down (absorption) for tow curve (green solid line and black solid line) with increasing SiO$_x$ concentration in the WL. Each curve has two peaks depending on the transitions taken (ground- and excited-state transitions). The wavelength shift is small for the ES peak. When SiO$_x$ concentration increases by **0**. **5**, the peak absorption in the TE mode increases with a wider red-shift (**170 nm**) in the peak wavelength, the transitions taken (ground- and excited-state transitions) each curve has two peaks depending on. The wavelength shift is small for the ES peak.

Figure 3 (A) shows gain curves for SiO$_x$ WL for four concentration undoped system. Gain is increase and shifted to upper change from absorption to gain at decrease SiO$_x$ –concentration in the WL. A comparison done in Table 1 shows that the main change in the spectrum is obtained by changing SiO$_x$ -mole fraction in the WL layer

The gain increment is small when SiO$_x$ -fraction in the WL is increased

The absorption spectra of the WL are measured to investigate their band gaps for two different SiO$_x$ -fraction in the WL concentrations in Si/SiO$_x$ samples. The direct allowed optical band gap Eg is estimated from the plots of (λ) versus (Gian 1/cm). As shown in the figure, the absorption spectrum of the Si/SiO$_x$ shows a in figure 3 (A),(B) and (C) when the concentrations are (0.25 and 0.35) , two peak gain range of 430 nm–530 nm.

Fig. 3 (B) p-type doped shows the gain for Si/SiO$_x$ system at different values from the concentrations. red solid line and blue solid line to upper to get the gain at decrease x mole fraction (0.11 and 0.15 compositions), while green solid line and black solid line to lower to get the gain at increase x mole fraction (0.25 and 0.35 compositions). The gain part is not included since there is not external signal input power (P_s=0). where they have peaks due to the ground (GS), first, and second excited state transitions.

Fig. 3 (C) **n**-type doped the gain have lower value compared by Fig. 3 (B) this mean p-type doped is upper the linear gain from n-typed doped, because the doped is the holes. The peak heights are doubled with doping. The peak wavelength appears at 420 nm and 400 nm they are still the same under doping. The first four structures peaked at the same wavelength and only differed in their gain value for undoped structures, and the GS and first ES gain values became the same under doping.

nm and 400 nm they are still the same under doping. The first four structures peaked at the same wavelength and only differed in their gain value for undoped structures, and the GS and first ES gain values became the same under doping.

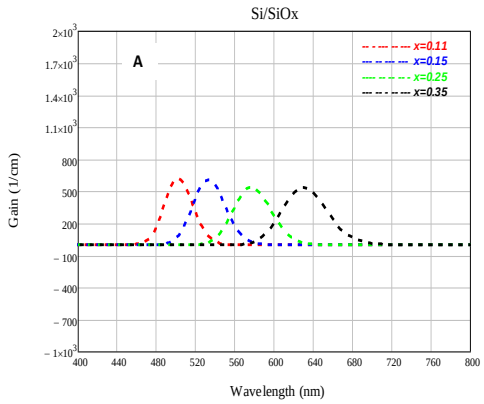

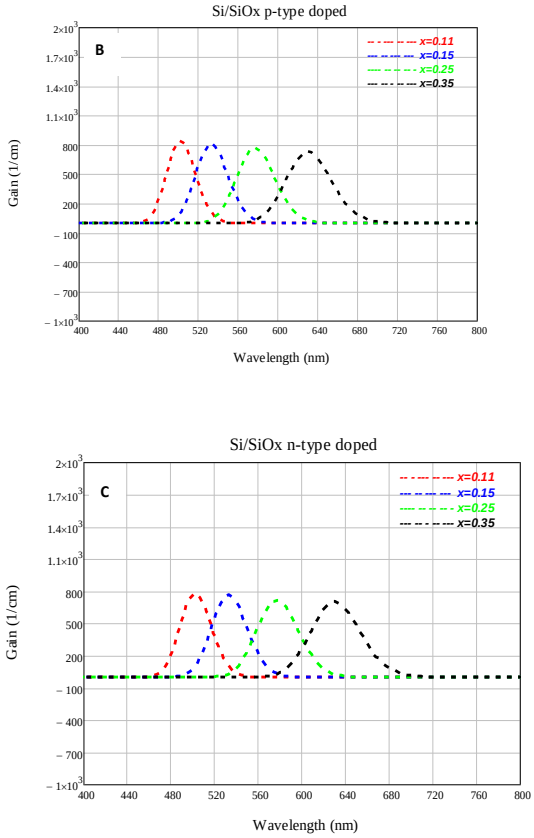

Figure 3: Calculated Gain Spectra at different values of, WL mole fraction for structure Si/SiO_x, (A) spectra of an undoped structure is dash line and (B) p-type (C) doped and n-type doped structure is solid line.

Fig. 4 shows Si/SiO_x doped QD structures at different injection carrier current, show at increase injection current density , the linear gain upper for black dash curve is high gain because increase injection carrier current while we show red dash line in absorption region due to lower injection current , at upper carrier density change the linear gain from absorption case to gain , one peak due to the ground (GS), first, The peak curve are increase with doped. The wavelength curve noted at 6.43, 1.26, and 6.83 μm, and they are still the equal under doped.

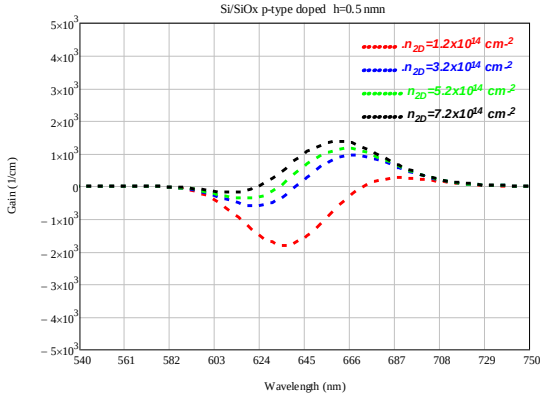

Figure 3: explain linear gain curves doped system Si/SiO_xat different injection current carrier concentration.

VII. Conclusions

The structure $Si/SiO_{0.25}$have two peaks from ES and GS transitions: 470 nm and 630 nm. The peaks of other structures studied here fall between them. Cd content reduces its peak wavelength. The results obtained are ascribed to the calculated discontinuity of the bands for each structure (mole fraction), which is one of the merits of this work. Doping is used to populate the ground state of holes, doubling the gain. The effect of QD size effect is also examined. The wavelength is extended by 20 nm for each 1 nm QD height increment. These visible bands are essential in different applications.

Disclosures. The authors declare no conflicts of interest

Funding: The authors declare that they have no funding.

Conflicts of interest/Competing interests: The authors declare that they have no conflicts of interest.

Availability of data and material: The data used are placed in the text of this work.

Author's contribution: The authors contributed equally.

Ethics approval: The work has not been sent to any other site.

Consent to participate: All the Authors Consent to participate.

Consent for publication: All the authors consent to publication

References

[1] F. M. Abdel-Awwad, Mohamed, "Optical Gain Experiment Manual," no. October, 2012.

[2] L. Amplification and S. Emission, *12 Optical Gain and Lasers*. 2019.

[3] J. PIPREK, "Photon Generation," *Semicond. Optoelectron. Devices*, pp. 121–139, 2003, doi: 10.1016/b978-0-08-046978-2.50030-2.

[4] M. J. Connelly, "Nonlinear Fiber Optics, 2nd edn, Ch. 8-10," *Fiber nonlinearities Opt. communications. Opt. Quantum Electron.*, vol. 19, no. 8, pp. 1–17, 1992.

[5] S. Dutta and P. Dutta, "Silicon – A Versatile Material," *Sci. Report.*, vol. 1, no. February, pp. 40–42, 2010.

[6] Z. Kang, Y. Liu, and S. T. Lee, "Small-sized silicon nanoparticles: New nanolights and nanocatalysts," *Nanoscale*, vol. 3, no. 3, pp. 777–791, 2011, doi: 10.1039/c0nr00559b.

[7] H. Chang and S. Q. Sun, "Silicon nanoparticles: Preparation, properties, and applications," *Chinese Phys. B*, vol. 23, no. 8, pp. 1–14, 2014, doi: 10.1088/1674-1056/23/8/088102.

[8] D. Bimberg, "Quantum dots for lasers, amplifiers

and computing," no. January 2004, pp. 2–2, 2004, doi: 10.1109/cleopr.2003.1274486.

[9] A. P. Alivisatos, "Downloaded from www.sciencemag.org on March 4 , 2011 Downloaded from www.sciencemag.org on March 4 , 2011," *Dots. Sci.*, pp. 933–937, 1996.

[10] M. Odeh, "About the Quantum Mechanics of the Electrons in Crystal Lattices Historical Background : Bloch Wave Theorem :," p. 555, 2018.

[11] K. Agarwal, H. Rai, and S. Mondal, "Quantum dots: an overview of synthesis, properties, and applications," *Mater. Res. Express*, vol. 10, no. 6, 2023, doi: 10.1088/2053-1591/acda17.

[12] J. P. M. Pacheco, A. Carballar, and G. Cincotti, "Quantum Dot Lasers na :," 2005.

[13] J. Kim, M. Laemmlin, C. Meuer, D. Bimberg, and G. Eisenstein, "Static gain saturation model of quantum-dot semiconductor optical amplifiers," *IEEE J. Quantum Electron.*, vol. 44, no. 7, pp. 658–666, 2008, doi: 10.1109/JQE.2008.922325.

[14] M. Abdullah, B. O. Al-Nashy, and A. H. Al-Khursan, "Optical gain of CdxZn1−xTe quantum dot structures," *Micro Nano Lett.*, vol. 18, no. 9–12, 2023, doi: 10.1049/mna2.12180.

[15] J. Kim and S. L. Chuang, "Theoretical and experimental study of optical gain, refractive index change, and linewidth enhancement factor of p-doped quantum-dot lasers," *IEEE J. Quantum Electron.*, vol. 42, no. 9, pp. 942–952, 2006, doi: 10.1109/JQE.2006.880380.

[16] M. H. Mokhilif, "Linear Modal Optical Gain in Quantum Dot Semiconductor Optical Amplifiers".

[17] N. N. Ledentsov *et al.*, "Quantum-dot heterostructure lasers," *IEEE J. Sel. Top. Quantum Electron.*, vol. 6, no. 3, pp. 439–451, 2000, doi: 10.1109/2944.865099.

[18] J. N. Jabir, S. M. M. Ameen, and A. H. Al-Khursan, "Plasmonic Quantum Dot Nanolaser: Effect of 'Waveguide Fermi Energy,'" *Plasmonics*, vol. 14, no. 6, pp. 1881–1891, 2019, doi: 10.1007/s11468-019-00981-2.

[19] B. Al-Nashy, A. G. Al-Shatravi, M. Abdullah, and A. H. Al-Khursan, "InTlSb quantum dot structures," *Results Phys.*, vol. 12, no. January, pp. 1492–1494, 2019, doi: 10.1016/j.rinp.2019.01.039.

[20] M. Abdullah, B. O. Al-Nashy, and A. H. Al-Khursan, "Optical gain of CdxZn1−xTe quantum dot structures," *Micro Nano Lett.*, vol. 18, no. 9–12, pp. 1–6, 2023, doi: 10.1049/mna2.12180.

[21] P. C. Ku, C. J. Chang-Hasnain, and S. L. Chuang, "Slow light in semiconductor heterostructures," *J. Phys. D. Appl. Phys.*, vol. 40, no. 5, 2007, doi: 10.1088/0022-3727/40/5/R01.